Plasminogen Activator Inhibitor-1 Gene-deficient Mice

I. Generation by Homologous Recombination and Characterization

Peter Carmeliet,*‡ Lena Kieckens,*‡ Luc Schoonjans,‡ Beverly Ream,* Ann Van Nuffelen,*‡ George Prendergast,§ Michael Cole,§ Roderick Bronson,|| Désiré Collen,‡ and Richard C. Mulligan*

**Whitehead Institute for Biomedical Sciences, Cambridge, Massachusetts 02139-4307; ‡Center for Molecular and Vascular Biology, University of Leuven, B-3000 Leuven, Belgium; §Department of Molecular Biology, Princeton University, Princeton, New Jersey 08540; and ||Tufts University, School of Veterinary Medicine, Boston, Massachusetts 02111*

Abstract

Homozygous plasminogen activator inhibitor-1 (PAI-1)-deficient (PAI-$1^{-/-}$) mice were generated by homologous recombination in D_3 embryonic stem cells. Deletion of the genomic sequences encompassing the transcription initiation site and the entire coding regions of murine PAI-1 was demonstrated by Southern blot analysis. A 3.0-kb PAI-1-specific mRNA was identified by Northern blot analysis in liver from PAI-1 wild type (PAI-$1^{+/+}$) but not from PAI-$1^{-/-}$ mice. Plasma PAI-1 levels, measured 2-4 h after endotoxin (2.0 mg/kg) injection were 63±2 ng/ml, 30±10 ng/ml, and undetectable (< 2 ng/ml) in PAI-$1^{+/+}$, heterozygous (PAI-$1^{+/-}$) and PAI-$1^{-/-}$ mice, respectively (mean±SEM, n = 4-11). PAI-1-specific immunoreactivity was demonstrable in kidneys of PAI-$1^{+/+}$ but not of PAI-$1^{-/-}$ mice. SDS-gel electrophoresis of plasma incubated with ^{125}I-labeled recombinant human tissue-type plasminogen activator revealed an ~ 115,000-M_r component with plasma from endotoxin-stimulated (0.5 mg/kg) PAI-$1^{+/+}$ but not from PAI-$1^{-/-}$ mice, which could be precipitated with a polyclonal anti-PAI-1 antiserum. PAI-$1^{-/-}$ mice were viable, produced similar sizes of litters as PAI-$1^{+/+}$ mice, and showed no apparent macroscopic or microscopic histological abnormalities. (*J. Clin. Invest.* 1993. 92:2746-2755.) Key words: embryonic stem cells • gene targeting • development • fertility• fibrinolysis

Introduction

The fibrinolytic system has been claimed to play a role in a variety of biological phenomena (1, 2). Activation of plasminogen by tissue-type plasminogen activator (t-PA)[1] is believed to be responsible not only for fibrin-specific clot lysis and maintenance of vascular patency (2), but it is also believed to be involved in ovulation (3-5), embryogenesis (6), and brain function (7). Plasmin generation by urokinase-type plasminogen activator (u-PA) is believed to play a role in a variety of tissue remodeling processes, such as embryo implantation and embryogenesis (3, 6, 8), angiogenesis (3, 9), inflammation (1), cell invasion, and metastasis (10).

Inhibition of the fibrinolytic system may occur at the level of plasmin, mainly by α_2-antiplasmin or at the level of the plasminogen activators by specific plasminogen activator inhibitors (PAIs) (11, 12). Of those, endothelial or type 1 PAI (PAI-1) appears to be the primary physiological inhibitor of plasminogen activation (11, 12). It inactivates both t-PA and two-chain u-PA by rapid formation of inactive 1:1 stoichiometric complexes. PAI-1 is synthesized in several tissues and its expression is highly regulated by various hormones and growth factors (12).

Despite extensive biochemical characterization, the role of PAI-1 in vivo is poorly documented. The evidence for its presumed role in hemostasis, thrombosis, and thrombolysis is discussed in the accompanying paper (13), but its role in other phenomena is less well documented. Several lines of evidence suggest that PAI-1 plays a role in gonadotropin-induced ovulation, healing of the ruptured follicle, and development of the corpus luteum (3, 4). PAI-1 may also modulate embryo implantation via expression in the invasive trophoblast (14) and in the decidua (8), where it may control excessive proteolysis. Serine protease inhibitors indeed suppress embryo implantation in rodents, supporting the implication of the fibrinolytic system in this phenomenon (15).

To obtain new information on the role of PAI-1 in vivo, we have disrupted the PAI-1 gene in mice by homologous recombination in embryonic stem cells, whereby the entire coding region was deleted, and we have investigated its effects on organ development and reproduction.

Methods

Animals and blood collection. The mice were kept in microisolation cages on a 12-h day/night cycle and were fed a regular chow. Unless otherwise stated, the mice were anesthetized by intraperitoneal injection of 60 mg/kg Nembutal (Abbott Laboratories, North Chicago, IL), and blood was collected by vena cava puncture with a 24-gauge needle.

Construction of the gene targeting vector. The PAI-1 gene was isolated from a BALB/c genomic library (Clontech Laboratories, Palo Alto, CA) (Prendergast, G., and M. Cole); 8.1 kb of total homology was included in the parental pNT-vector that contains a neomycin and a Herpes simplex virus thymidine kinase expression cassette (16), as schematically represented in Fig. 1. Initially, a 4.5-kb SalI-XhoI fragment from plasmid pX5.4, containing the 5'-flanking XbaI-XhoI genomic sequences, was ligated into the XhoI-site of the pNT vector to produce pNT.PAI5' (not shown). The XhoI-site is ~ 1.0 kb upstream of the transcription initiation site of the PAI-1 promoter. In a second step, the 3.6-kb BamHI-EcoRI fragment from plasmid pH4, contain-

Part of this study has been published in abstract form (1993. *Ann. Hematol.* 66[Suppl. 1]:170).

Address correspondence to R. C. Mulligan, Ph.D., Whitehead Institute for Biomedical Sciences, 9 Cambridge Center, Cambridge, MA 02139-4307, or D. Collen, M.D., Ph.D., Center for Molecular and Vascular Biology, University of Leuven, Campus Gasthuisberg, O & N, Herestraat 49, B-3000 Leuven, Belgium.

Received for publication 21 June 1993 and in revised form 16 August 1993.

1. *Abbreviations used in this paper:* ES, embryonic stem (cell); FIAU, 1-[2-deoxy, 2-fluoro-β-D-arabinofuranosyl]-5-iodouracil; FIAU^R, FIAU resistant; G418, Geneticin; G418^R, G418 resistant; PAI-1, murine plasminogen activator inhibitor-1; PAI-$1^{+/+}$, wild type PAI-1 mice; PAI-$1^{+/-}$, heterozygous PAI-1-deficient mice; PAI-$1^{-/-}$, homozygous PAI-1-deficient mice; rPAI-1, recombinant murine plasminogen activator inhibitor-1; rt-PA, recombinant human t-PA; t-PA, tissue-type plasminogen activator; u-PA, urokinase-type plasminogen activator.

J. Clin. Invest.

0021-9738/93/12/2746/10 $2.00
Volume 92, December 1993, 2746-2755

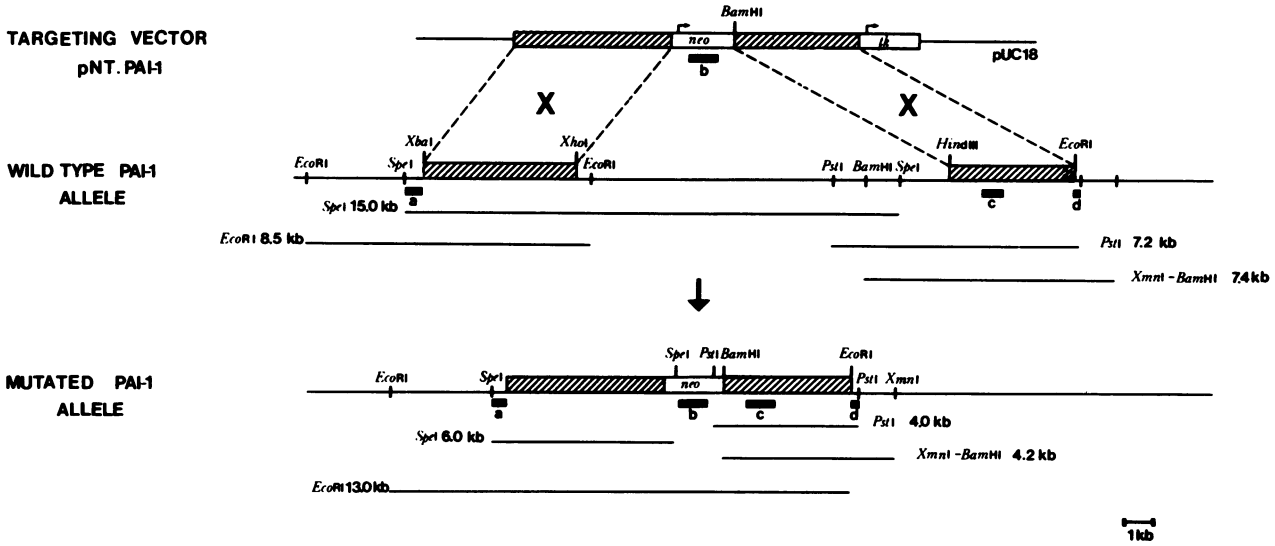

Figure 1. Outline of the strategy used to disrupt the murine PAI-1 gene. Schematic representation of the targeting vector pNT.PAI-1 used for the disruption of the PAI-1 gene, of the wild type PAI-1 allele, and of the homologously recombined allele. The targeting vector contains the neomycin resistance gene (*neo*) and the Herpes simplex virus thymidine kinase gene (*tk*) to allow for double selection of homologous recombinant events (33). Expression of the *neo* and *tk* genes was under the control of the phosphoglycerokinase promoter (16). Transcription of both resistance genes was in the same direction as the endogenous PAI-1 gene. The neo gene, inserted between the XhoI site in the PAI-1 promoter region and the HindIII site in the last exon, replaces the genomic sequences encompassing all coding regions of PAI-1. Upon homologous recombination, the disrupted PAI-1 allele acquires an additional BamHI site. The expected restriction fragments of the wild type and the targeted mutated allele are indicated with their relative sizes by underlining. Black bars denote the probes used for Southern blotting. Hatched bars represent the 5′ and 3′ flanks used for homologous recombination.

ing the 3′-flanking HindIII-EcoRI genomic sequences, was cloned into the BamHI-EcoRI restricted pNT.PAI5′ to generate pNT.PAI-1 (Fig. 1). As a result of the cloning strategy, a novel BamHI site downstream of the neomycin gene would be generated upon recombination of the targeting vector at the PAI-1 locus in the embryonic stem cells. The upstream HindIII site in the 3′-flanking region is located at basepair 2,636 of the PAI-1 cDNA, 1,297 bp downstream of the stop codon (17). As such, the neomycin expression cassette in the gene targeting vector was flanked by 5′- and 3′-untranslated PAI-1 sequences, but the vector did not contain the transcription initiation site nor any of the coding sequences of PAI-1.

Embryonic stem cell culture and transfection. D_3 embryonic stem cells (18) (obtained from R. Hynes, Massachusetts Institute of Technology, Cambridge, MA), were cultured (19) in embryonic stem cell medium (Dulbecco's modified Eagle's medium containing 4.5 g/liter glucose; Hazleton Laboratories, Lenexa, KS) and 15% heat-inactivated fetal bovine serum (Hyclone Laboratories, Salt Lake City, UT) supplemented with nonessential amino acids (GIBCO BRL, Gaithersburg, MD), 2 mM glutamine (GIBCO BRL), 0.1 mM β-mercaptoethanol (Sigma Immunochemicals, St. Louis, MO), 100 U/ml penicillin/0.1 mg/ml streptomycin, and 1,000 U/ml recombinant leukemia inhibitory factor (Esgro; GIBCO BRL). The cells were grown on lethally irradiated (1,500 rad for 30 min) primary mouse embryonic fibroblasts, prepared from neomycin-resistant, β_2m-deficient mice (provided by R. Jaenisch, Whitehead Institute, Cambridge, MA). Approximately 10^8 embryonic stem cells were electroporated with an electroporator from Bio-Rad Laboratories (Richmond, CA) (400 V, 25 μF, room temperature) with 100 μg of NotI-linearized targeting vector in electroporation buffer (20 mM Hepes buffer, pH 7.2, containing 6 mM dextrose, 0.7 mM Na_2HPO_4, 5 mM KCl, 137 mM NaCl, and 0.1 mM β-mercaptoethanol).

The cells were plated immediately after DNA transfer on 90-mm cell culture dishes containing embryonic fibroblast feeder layer cells, and selection was started 24 h later with 300 μg/ml G418 (Geneticin; GIBCO BRL) and 0.2 μM FIAU (1-[2-deoxy, 2-fluoro-β-D-arabinofuranosyl]-5 iodouracil, Bristol-Meyers Squibb, Princeton, NJ). 5 d later, selection was continued with 300 μg/ml G418 only. After 8–10 d in selection medium, visible colonies were isolated and transferred to 48-well cell culture dishes. At confluency, 80% of the cells of each 48-well cell culture dish were frozen in embryonic stem cell culture medium containing 10% DMSO, and the remaining cells were grown in 24-well cell culture dishes for genomic Southern blot analysis carried out as described below.

Generation of chimeric and PAI-1 deficient mice. Targeted clones containing a disrupted PAI-1 gene were injected into C57BL/6J (Jackson Laboratories, Bar Harbor, ME) host blastocysts as described by Bradley (20). Injected embryos were transferred into pseudopregnant $B6D_2F_1$ (Jackson Laboratories) foster mothers. Generated chimeric animals were back-crossed to C57BL/6J mice and germline transmission of embryonic stem cell DNA was scored by coat pigment. Heterozygous PAI-1–deficient mutants were identified by Southern blot analysis of tail tip genomic DNA as described below. Brother-sister mating was carried out to generate homozygous PAI-1–deficient mutants.

Southern blot analysis of genomic DNA. DNA was isolated from cultured cells and mouse tail tips as previously described (21). Briefly, cells or tail tips were incubated overnight in lysis buffer (1% SDS, 500 or 100 μg/ml, respectively, of proteinase K, 100 mM NaCl, 1 mM EDTA, 10 mM Tris.HCl buffer, pH 7.5), at 37°C (cultured cells) or 55°C (tail tips) and genomic DNA was spooled after precipitation with an equal volume of isopropylalcohol. Embryonic stem cell and tail tip DNA was digested with the indicated restriction enzymes and analyzed by genomic Southern blotting procedures as described elsewhere (22).

To screen for embryonic stem cell colonies harboring a recombined PAI-1 gene, a SpeI-XbaI probe (Fig. 1, probe *a*) was used, which encompasses a 700-bp genomic fragment adjacent to the 5′ XbaI-XhoI fragment of the targeting construct. This 5′ external probe detects a 8.5-kb EcoRI fragment of the wild type allele and a 13.0-kb EcoRI fragment of the mutated allele, and a 15.0-kb SpeI fragment of the wild type and the 6.0-kb SpeI fragment of the mutated allele.

To document correct homologous recombination at the 3′ end, a 550-bp NheI fragment of the 3′ HindIII-EcoRI flank used in the targeting construct (Fig. 1, probe *c*), and a 200-bp HindIII-PstI fragment

adjacent to the 3′ HindIII-EcoRI targeting flank (Fig. 1, probe *d*) were used. These probes detect a 7.2-kb PstI fragment of the wild type and a 4.0-kb PstI fragment of the mutated allele, and a 7.4-kb XmnI-BamHI fragment of the wild type and a 4.2-kb XmnI-BamHI fragment of the mutated allele. To exclude additional random integration of the targeting vector, a 600-bp PstI fragment of the neomycin gene (Fig. 1, probe *b*) was used, which detects a 13.0-kb EcoRI fragment of the homologously recombined gene.

Northern blot analysis. Total RNA from liver of wild type (PAI-$1^{+/+}$) and homozygous PAI-I–deficient (PAI-$1^{-/-}$) mice, pretreated 4 h earlier with 0.5 mg/kg endotoxin (Difco Laboratories, Detroit, MI) was isolated with the guanidinium thiocyanate-phenol-chloroform single-step extraction method according to Chomczynski and Sacchi (23). 20 μg of denatured total RNA was separated by formaldehyde-agarose gel electrophoresis and bound to a Zetabind nylon membrane (Zetaprobe; Bio-Rad, Brussels, Belgium) by capillary transfer, using standard procedures (22). Blots were prehybridized for 6–12 h and hybridized for 48 h at 42°C in a hybridization solution containing 1.0 M Na-phosphate buffer, pH 7.2, containing 0.25 M NaCl, 7% (wt/vol) SDS, 1 mM EDTA, 50% formamide, 5% (wt/vol) dextran sulfate and 0.01 mg/ml denatured herring sperm DNA. After hybridization, blots were washed in 2 × SSC, containing 0.1% SDS for 2 × 5 min at room temperature, followed by two 30-min washes with 0.5 × SSC containing 0.1% SDS, at 65°C. A 900-bp NcoI-HindIII fragment of the PAI-1 cDNA (17) was used as a probe.

Expression and purification of PAI-1 and production of antibodies. The PAI-1 expression vector was constructed as follows: A 1,074-bp PstI-DraI fragment (PstI site at basepair 340, DraI site at basepair 1,414, numbering according to reference 17), of which the DraI site was HindIII-linkered, was cloned into pGEM-4Z (Promega Biotec, Madison, WI) to yield pGEM-mPAIPsh. This plasmid contains part of the PAI-1 coding sequence and 74 bp of 3′-untranslated PAI-1 sequence. To obtain cytoplasmic expression, an ATG codon was introduced by PCR mutagenesis in front of the Leu^{24}-codon of the presumed NH_2-terminal residue of mature PAI-1, as deduced by alignment of the murine PAI-1 cDNA sequence with the human PAI-1 cDNA sequence (24). Mutagenesis was performed using PCR with full-length PAI-1 cDNA and the GAGAGGGATCCATGTTACCCCTCCGAGAAT (the engineered ATG codon upstream of nucleotides 201–216 is underlined) and ATAGCATCTTGGATCTG (nucleotides 385–369) primers. After digestion with BamHI and PstI, the restricted PCR product containing the ATG codon and 140 nucleotides of PAI-1 coding sequence up to the PstI site at basepair 340, was ligated with a 1,076-bp PstI-HindIII fragment from pGEM-mPAIPsh, containing the remainder of the PAI-1 coding sequence, and with the BamHI-HindIII–linearized plasmid pMC5-19 (25), to yield pMCPAI-PCR15. Mutagenesis was confirmed by sequencing of the final expression plasmid. After cotransfection of the expression plasmid pMCPAI-PCR15 and pUBS520 (25) (obtained from S. Fisher, Boehringer Mannheim GmbH, Mannheim, Germany) into *Escherichia coli* WK6 cells (25), chloramphenicol-resistant (50 μg/ml), and kanamycin-resistant (70 μg/ml) bacterial clones were cultivated in liquid culture. Recombinant PAI-1 (rPAI-1) expression was induced by adding isopropylthio-β-D-galactoside (1 mM final concentration). After 4 h, *E. coli* cells were centrifuged for 15 min at 3,500 rpm and at 4°C, and the cell pellet was resuspended in 10 ml 25% sucrose, 15 mM Na-phosphate buffer, pH 6.0, to which the following reagents were added: 5 ml 0.25 M EDTA, 5 μl aprotinin (750 U/ml), 5 μl leupepsin (10 mg/ml), 260 μl PMSF (10 mg/ml), 26 μl DTT (10 mg/ml), 26 μl pepstatin A (0.7 mg/ml), 26 μl benzamidine/HCl (1 mM), 26 μl antipain (10 mg/ml), and 8 ml of a solution containing 0.2% Nonidet P-40, 0.25 mM EDTA, and 50 mM Na-phosphate buffer, pH 6.0. After incubation for 10 min on ice, cells were sonicated on ice for 3 min with a sonifier (model no. 250, position no. 8; Branson Ultrasonics Corp., Danbury, CT), and the lysate was centrifuged at 20,000 rpm for 20 min at 4°C.

Recombinant murine PAI-1 (rPAI-1) from *E. coli* lysates was purified as described by Seetharam et al. (26) with minor modifications. Briefly, the *E. coli* supernatant (~ 200 ml) was passed through a Q-Sepharose column (2.5 × 10 cm) (Pharmacia, Uppsala, Sweden) equilibrated with 0.1 M NaCl, 0.05 M Na-phosphate buffer, pH 7.5, at a flow rate of 25 ml/h. The rPAI-1 containing flow through from the Q-Sepharose column was adjusted to pH 6.0 and dialyzed against 0.1 M NaCl, 0.05 M Na-phosphate buffer, pH 6.0, before loading onto an SP-Sepharose column (2.5 × 12 cm) (Pharmacia) equilibrated with 0.1 M NaCl, 0.05 M Na-phosphate buffer, pH 6.0, at a flow rate of 30 ml/h. rPAI-1 was eluted from the column using 0.05 M Na-phosphate buffer, pH 8.0. rPAI-1 containing fractions were collected into 1 M acetate buffer, pH 4.5 (1/10 vol). Pooled fractions were adjusted to 0.3 M NaCl and to pH 5.5 and loaded onto a heparin-Sepharose column (0.9 × 15 cm) (Pharmacia) equilibrated with 0.3 M NaCl, 0.05 M acetate buffer, pH 5.5, at a flow rate of 10 ml/h. The bound rPAI-1 was then eluted using a NaCl gradient (0.3–1.1 M) in 0.05 M acetate buffer, pH 5.5. The purified material migrated as a single component with an apparent relative molecular mass of 45 kD on SDS-gels and reacted with anti–human PAI-1 antibodies on Western blotting (data not shown). The purified rPAI-1 was primarily obtained in the latent form, with a specific activity of 7,000 U/mg (representing ~ 1% of the theoretical maximal specific activity calculated on the basis of a specific activity for t-PA of 500,000 U/mg and relative molecular mass of 70,000 and 45,000 for recombinant human t-PA (rt-PA) and rPAI-1, respectively). The rPAI-1 could be reactivated by incubation with urea or guanidium hydrochloride according to the method of Hekman and Loskutoff (27). After reactivation and extensive dialysis against cold phosphate-buffered saline (0.04 M phosphate, 0.14 M NaCl, pH 7.4), the reactivated rPAI-1 had a specific activity of 180,000 U/mg.

Antibodies against purified rPAI-1 were produced by immunization of rabbits. The IgG fraction, purified by chromatography on Protein A Sepharose (Pharmacia) recognized the 45-kD murine and the 50-kD human PAI-1 on Western blotting (data not shown). Alternatively, murine monoclonal antibodies raised against human PAI-1 were screened for their cross-reactivity with murine PAI-1. Out of 81 antibodies, 24 were found to exhibit significant cross-reactivity.

Histopathologic examination. Three PAI-$1^{+/+}$ and three PAI-$1^{-/-}$ mice of either sex, aged 7 mo, were killed with an overdose of Avertin (2,2,2-tribromoethanol; Aldrich Chemie, Bornem, Belgium) and perfusion-fixed with cold 10 mM Na-phosphate buffer, pH 7.4, followed by Bouin's fixative. Whole fixed mice were postfixed in Bouin's fixative until use. Representative sections of all tissues were selected for histopathological examination. The tissues included five cross sections of brain, two cross sections of spine with spinal cord, a section of knee with leg muscle, lung, heart, kidney, liver, intestinal tissues, stomach, reproductive organs, thyroid, adrenal, eye, and pancreas.

Immunocytochemistry. Male and female mice were anesthetized with a mixture of Rompun (Bayer, Leverkusen, Germany) and Ketalar (Warner-Lambert, Zaventem, Belgium) and perfusion-fixed with cold (4°C) 0.01 M Na-phosphate buffer, pH 7.4, followed by 1% (wt/vol) paraformaldehyde in 0.1 M Na-phosphate buffer, pH 7.4. Tissues were dissected and immediately (without postfixation) submerged for 36 h in 0.1 M Na-phosphate buffer, pH 7.4, containing 20% (wt/vol) sucrose. Tissues were then frozen in liquid 2-methylbutane, and cryostat sections (15–25 μm) were produced at −26°C and were mounted on chromealum-gelatin-coated slides. Cryostat sections were soaked in 0.01 M Tris/HCl buffer, pH 7.6, containing 0.15 M NaCl and 0.1% (vol/vol) Triton X-100 (TBS-Triton) for 10 min, exposed to 20% normal goat serum (Department of Zoology, University of Leuven, Belgium) for 45 min, briefly rinsed in TBS-Triton, and exposed to varying concentrations of rabbit anti–PAI-1 antibodies obtained as described above, or of rabbit anti–human PAI-1 antibodies (American Diagnostica Inc., Greenwich, CT). Optimal IgG concentrations for staining were found to be 1–2 μg/ml when incubated at room temperature for 14 h. After incubation, the slides were treated with goat anti–rabbit IgGs (diluted 1:20 in TBS-Triton) for 30 min at room temperature, and then with rabbit peroxidase/antiperoxidase complexes (diluted 1:300 in TBS-Triton) for 30 min at room temperature. Peroxidase activity was revealed with 3,3′-diamino benzidine tetrahydrochloride

(25 mg dissolved in 200 ml 0.05 M Tris/HCl buffer, pH 7.6, containing 75 μl of 30% hydrogen peroxide). Between incubations, the sections were rinsed extensively with TBS-Triton. Controls included (*a*) omission of either the first, second, or third layer of antiserum; and (*b*) absorption of the primary rabbit anti-PAI-1 antibodies with highly purified recombinant human PAI-1, coupled to CNBr-activated Sepharose beads, as described below.

PAI activity. PAI activity in plasma samples was determined according to Verheijen et al. with minor modifications (28). Briefly, samples were diluted at least twofold in 0.05 M Tris/HCl, 0.1 M NaCl buffer, pH 7.4, containing 0.01% Triton X-100, (Tris-buffer) and incubated for 5 min at 37°C with an equal volume of rt-PA (20 IU/ml). The samples were then acidified with an equal volume of 0.16 M HCl, incubated for 10 min at room temperature, followed by addition of 1 vol of 0.16 M NaOH and 7 vol of Tris-buffer. This procedure resulted in neutralization of most of the plasmin inhibitor activity in plasma. Then 100 μl of this mixture was incubated in the wells of a microtiter plate with an equal volume of a solution containing plasminogen (final concentration 1 μM), CNBr-digested fibrinogen (final concentration 1 μM), and S-2251 (final concentration 0.6 mM). Residual rt-PA activity was quantified by recording the change in absorbance at 405 nm. 1 U PAI-1 was defined as the amount that inhibited 1 IU of rt-PA.

Active PAI-1 levels were also determined using a monoclonal antibody-based immunofunctional assay, specific for the PAI-1/rt-PA complex (29). MA-16F11, a monoclonal antibody raised against human PAI-1, which cross-reacted for ~ 30% with the recombinant murine PAI-1 (rPAI-1) was used for capture, and a monoclonal antibody directed against rt-PA (MA-62E8), which did not (< 1%) cross-react with murine t-PA, was conjugated to horseradish peroxidase and used for tagging. Alternatively, MA16F11 was replaced by polyclonal rabbit anti-PAI-1 antibodies, yielding similar results (data not shown).

Immunoprecipitation of PAI-1 in plasma samples was achieved by mixing 50 μl plasma with 20 μl CNBr-activated Sepharose beads, to which rabbit anti-rPAI-1 was coupled (1.25 mg IgG/ml gel), for 2 h at room temperature, followed by removal of the beads by centrifugation. A rabbit antistaphylokinase antiserum coupled to Sepharose beads was used as a control antiserum.

Complex formation of PAI-1 with ^{125}I-rt-PA. Incubation of plasma samples with ^{125}I-rt-PA for generation of labeled PAI/rt-PA complexes was carried out as previously described (30). Briefly, plasma samples, obtained from mice injected 2 h previously with 0.5 mg/kg endotoxin were incubated with rt-PA, which was radiolabeled with ^{125}I using the Iodogen method. Active ^{125}I-rt-PA was added in slight molar excess of active PAI-1 (as determined by the method by Verheyen) to the 10-fold diluted plasma samples from PAI-1$^{+/+}$ mice. An equal amount of ^{125}I-rt-PA was added to the 10-fold diluted plasma from PAI-1$^{-/-}$ mice. After a 15-min incubation period at 37°C, the reaction was terminated by the addition of 0.25 vol of 50 mM Tris/HCl buffer, pH 8.0, containing 5 mM EDTA, 5% (wt/vol) SDS, 0.05% bromophenol blue, and heating for 30 s at 100°C. The mixtures were subjected to electrophoresis on a 10–15% gradient SDS-polyacrylamide gel. The relative position of the ^{125}I-label was visualized by autoradiography. The autoradiograms were intentionally overexposed to obtain maximal sensitivity. Immunoprecipitation of PAI-1 in plasma was carried out as described above in the section on PAI-1 activity.

Statistical analysis. The statistical significance of differences between groups was determined using Student's *t* test for paired or unpaired values and two-sided *P* values.

Results

Targeting of the PAI-1 gene

To target the murine PAI-1 gene, a replacement-type targeting vector was constructed, in which a neomycin-expression cassette replaced the genomic sequences encompassing the entire coding regions of PAI-1, as schematically represented in Fig. 1. Correct homologous recombination would, thus, result in a total absence of the PAI-1 protein. After electroporation of the linearized targeting construct in the D_3 line of embryonic stem cells (129 genetic background [18]), homologous integration was observed in 17 out of 340 (5%) double-resistant (G148^R-FIAU^R) clones that were analyzed by Southern blot analysis of genomic DNA (Table I). As shown in Table I, the enrichment obtained by double selection (G418 and FIAU) over the single selection (G418 only) ranged in two experiments between 4.9-fold and 6.0-fold. Genomic DNA from individual embryonic stem cell clones was digested with EcoRI and hybridized to probe a located adjacent to the 5′ side of the homology region present in the targeting construct (Fig. 1). Genomic DNA from wild type cells yielded a 8.5-kb fragment after EcoRI digestion, whereas the disrupted gene produced a 13.0-kb fragment (Fig. 2 *A*).

After expansion of clonal populations of embryonic stem cells containing the disrupted allele, additional Southern blot analyses were performed on genomic DNA digested with SpeI (hybridized with probe a), PstI, and XmnI-BamHI (hybridized with probe c [Fig. 1]) to confirm site-specific recombination at the PAI-1 locus (data not shown). Finally, hybridization of EcoRI-restricted genomic DNA with a neomycin-specific probe (Fig. 1, probe *b*) was used to reveal single integration of the targeting construct at the PAI-1 locus (Fig. 2 *B*), by exclusive generation of a 13.0-kb fragment from the targeted allele.

Germline transmission of the inactivated PAI-1 gene

Two independent clones that had undergone homologous recombination (clones P176 and P292) were then injected into C57BL/6J host blastocysts (Table II). With clone P292, the following chimeric animals were obtained: two males and one female with < 30% chimerism, one male and one female with 30–70% chimerism, and three males with > 90% chimerism. With clone P176, the corresponding numbers were: two males and one female with < 30% chimerism, three males and two females with 30–70% chimerism, three males and four females

Table I. Frequency of Gene Targeting

Experiment	Number of ES cells electroporated	Number of G418^R ES colonies	Number of G418^R and FIAU^R ES colonies	Enrichment factor (-fold)	Frequency of homologous recombinants in G418^R and FIAU^R colonies
1	1×10^7	1,020	208	4.9	ND
2	1×10^8	23,800	3,970	6.0	17/340 (5.0%)

Embryonic stem (ES) cells were transfected with linearized targeting vector as described in the text. G418^R, G418 resistant; FIAU^R, FIAU resistant. The enrichment factor is the ratio of the number of G418^R over G418^R/FIAU^R ES cell colonies. ND, not determined.

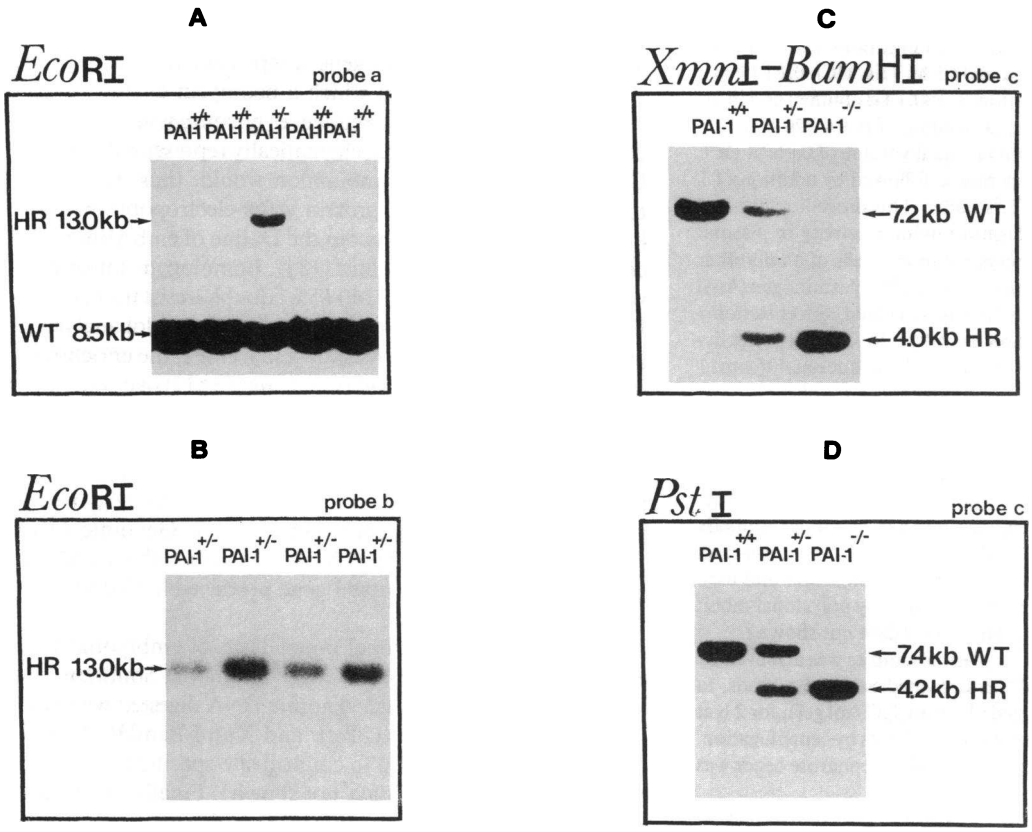

Figure 2. Southern blot analysis of genomic DNA. (*A*) Southern blot analysis of genomic DNA from D_3 embryonic stem cells, digested with EcoRI and hybridized to the 5′-PAI-1 flanking probe *a* (Fig. 1). The appearance of a novel 13.0-kb EcoRI fragment is indicative of a correctly targeted mutant allele. Genomic DNA from two individual embryonic stem cell clones was pooled and electrophoresed, resulting in the unequal intensity of the mutated versus the wild type allele fragment. (*B*) Southern blot analysis of genomic DNA from the homologously recombined embryonic stem cell clones, digested with EcoRI and hybridized with the *neo*-specific probe (Fig. 1, probe *c*). (*C* and *D*) Representative example of Southern blot analysis of genomic tail tip DNA from PAI-$1^{+/+}$, PAI-$1^{+/-}$, and PAI-$1^{-/-}$ mice (F_3 generation), digested with XmnI and BamHI (*C*) and with PstI (*D*), respectively. The PstI-digested and XmnI-BamHI–digested genomic DNA were hybridized with probe *c* (Fig. 1). WT, wild type; HR, homologously recombined.

with 70–90% chimerism, and twelve males and five females with > 90% chimerism. All these chimeras were tested for germline transmission of the mutated allele, which was obtained with three males obtained with clone P292 (P292-1A, P292-5B, and P292-5E), and one male and one female obtained with clone P176 (P176-12C and P176-13B). Thus, although a significant number of chimeric animals with > 90% coat color chimerism were obtained by injecting clone P176, only one male and one female chimera transmitted the mutation through the germline. Of the nongermline competent chimeras with > 90% chimerism, six males and two females were sterile, and two males and two females produced only one litter, despite continued breeding efforts for more than 8 mo.

To accelerate expansion of the PAI-1 transgenic colony, the initial heterozygous PAI-1–deficient (PAI-$1^{+/-}$) F_1 males were mated with several C57BL/6J wild type PAI-1 (PAI-$1^{+/+}$) females to produce more PAI-$1^{+/-}$ male and female F_2 offspring that had a genetic background of 25% of 129 and 75% of C57BL/6J. F_3 PAI-$1^{+/+}$ and homozygous PAI-1–deficient mice (PAI-$1^{-/-}$) littermates with the 25% of 129: 75% of C57BL/6J genetic background were used throughout the present study.

Viability, fertily, and growth of PAI-1 deficient mice

Heterozygous PAI-$1^{+/-}$ mice (F_2 generation) were intercrossed and their F_3 offspring were genotyped 3 wk after birth by

Table II. Frequency of Germline Transmission of Targeted ES Cell Lines

ES cell clone	Number of blastocysts injected	Number of live progeny	Number of chimeras		Number of chimeras with >90% chimerism		Number of germline transmitting chimeras	
			Males	Females	Males	Females	Males	Females
P292	150	48	6	2	3	0	3	0
P176	234	82	20	12	12	5	1	1

The individual ES cell clones were injected in the number of blastocysts indicated. Injected blastocysts were then transferred to pseudopregnant females and the number of live progeny and of chimeras determined. The number of chimeras transmitting the mutated allele through the germline is also indicated.

Table IIIA. Genotype Distribution of 3 wk-old Littermates

	PAI-1$^{+/+}$		PAI-1$^{+/-}$		PAI-1$^{-/-}$		Total
	n	Percent	*n*	Percent	*n*	Percent	*n*
Male	96	(30)	162	(50)	66	(20)	324
Female	68	(23)	152	(51)	79	(26)	299
Total	164	(26)	314	(50)	145	(23)	623

F_3 littermates, obtained by mating F_2 PAI-1$^{+/-}$ mice with a 25% of 129 and a 75% of C57BL/6J genetic background (see text) were genotyped by Southern blot analysis of genomic tail tip DNA.

Southern blot analysis of tail tip DNA, digested with XmnI and BamHI or with PstI. A representative example of such a Southern blot analysis of genomic DNA, restricted with XmnI and BamHI (Fig. 2 *C*) or with PstI (Fig. 2 *D*) from PAI-1$^{+/+}$, PAI-1$^{+/-}$, and PAI-1$^{-/-}$ littermates is shown. Among the 623 F_3 offspring tested, 164 were PAI-1$^{+/+}$ (26.3%), 314 were PAI-1$^{+/-}$ (50.4%), and 145 were PAI-1$^{-/-}$ (23.3%) (Table III *A*). This distribution is not significantly different (chi-square test) from the expected 1:2:1 frequencies assuming equal viability of PAI-1$^{+/+}$, PAI-1$^{+/-}$, and PAI-1$^{-/-}$ mice.

Also, PAI-1 deficiency did not significantly alter the growth of young animals; at 4 wk of age, the weight of PAI-1$^{-/-}$ and PAI-1$^{+/+}$ mice were similar (15.7±0.4 g (n = 11) vs 16.4±0.5 g (n = 7), P = 0.31).

PAI-1$^{-/-}$ mice were intercrossed to document the effect of PAI-1 gene disruption on reproduction. As shown in Table III *B*, F_3 PAI-1$^{-/-}$ mice produced similar sizes and numbers of litter (F_4 generation) as F_3 PAI-1$^{+/+}$ mice. It appears, thus, that disruption of the PAI-1 gene did not significantly influence viability, fertility, or development.

Table IIIB. Size and Frequency of Litters from F_3 PAI-1 Breeding Pairs

	PAI-1$^{+/+}$	PAI-1$^{-/-}$
Size of litters (mice per litter)	7.3±0.5 (28)	6.2±0.4 (39)
Time between litters (d)	33±2 (25)	33±4 (15)

Size and frequency of litters from F_3 PAI-1$^{+/+}$ and F_3 PAI-1$^{-/-}$ breeding pairs. The results represent mean±SEM of the number of data points indicated between brackets.

Histological examination

No significant histological abnormalities could be documented on microscopic examination of the tissues listed in the methods section. No signs of bleeding were observed in any of the tissues in PAI-1$^{-/-}$ mice. The oldest PAI-1$^{-/-}$ mice presently available are 11 mo old and still appear healthy.

RNA analysis

Northern blot analysis of RNA prepared from liver of PAI-1$^{+/+}$ and PAI-1$^{-/-}$ mice, pretreated 4 h earlier with 0.5 mg/kg endotoxin, hybridized with a PAI-1–specific cDNA probe, revealed the specific 3.0-kb mRNA in PAI-1$^{+/+}$ mice, while no such mRNA could be detected in the PAI-1$^{-/-}$ mice (Fig. 3 *A*). Rehybridization of the same blot with the neomycin-specific probe revealed the presence of a 1.3-kb neomycin mRNA in the PAI-1$^{-/-}$, but not in the PAI-1$^{+/+}$ mice (Fig. 3 *B*).

Immunocytochemical analysis of PAI-1

Cryostat sections of the kidneys of PAI-1$^{+/+}$ and PAI-1$^{-/-}$ mice were stained with a polyclonal rabbit anti–PAI-1 antiserum, which recognized purified rPAI-1 on a Western blot (data not shown). Very weak PAI-1 immunoreactivity was ob-

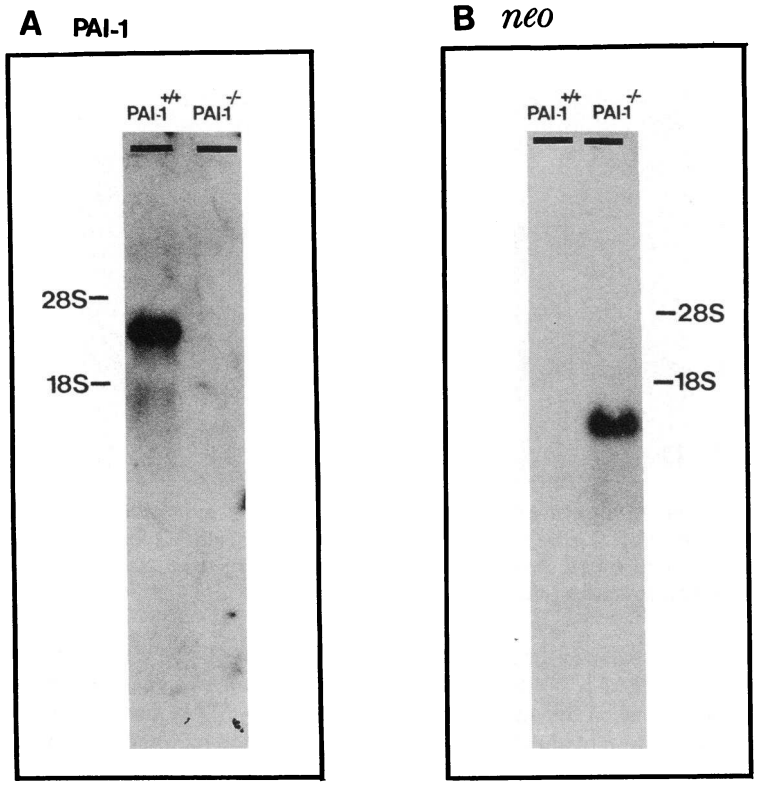

Figure 3. Northern blot analysis of RNA from liver after endotoxin stimulation of the mice. 20 μg of total RNA, prepared from liver was analyzed by Northern blot analysis using a PAI-1–specific probe (*A*) or a neomycin-specific probe (*neo*) (*B*). In PAI-1$^{+/+}$ mice, a 3.0-kb PAI-1–specific mRNA is present, which is not detectable in PAI-1$^{-/-}$ mice. Conversely, a ~ 1.3-kb *neo*-specific mRNA was only present in RNA from PAI-1$^{-/-}$ mice.

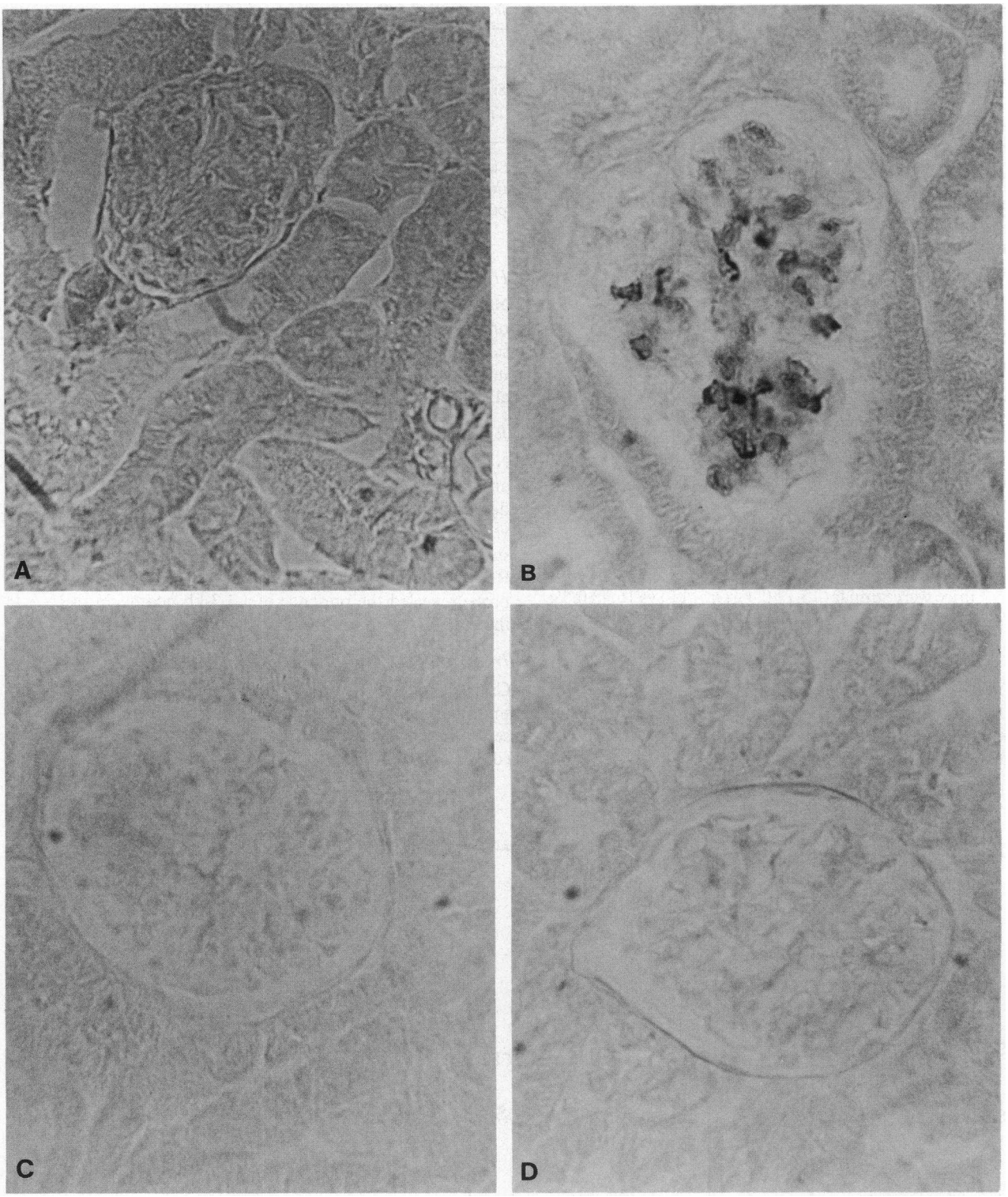

Figure 4. Immunostaining using polyclonal rabbit anti–PAI-1 antibodies of cryostat sections of kidneys from PAI-$1^{+/+}$ mice without (*A*) and with an intraperitoneal injection of 0.5 mg/kg endotoxin (*B*) and from PAI-$1^{-/-}$ mice pretreated with 0.5 mg/kg endotoxin (*C*). In *D*, a section of an endotoxin stimulated PAI-$1^{+/+}$ mouse stained with preabsorbed antiserum is shown. The PAI-1 reactivity appears to be localized in the juxtaglomerular apparatus (without endotoxin, *A*) and in the glomerular structures (after induction by endotoxin, *B*).

served in structures, tentatively identified as the juxtaglomerular apparatus in the kidneys of PAI-$1^{+/+}$, but not of PAI-$1^{-/-}$ mice (Fig. 4 *A*; only PAI-$1^{+/+}$ mice are shown). Intraperitoneal injection of endotoxin (2 mg/kg) 4 h before killing the animals revealed substantial induction of PAI-1 immunoreactivity in the glomeruli of PAI-$1^{+/+}$ mice (Fig. 4 *B*), but not of PAI-$1^{-/-}$ littermates (Fig. 4 *C*) (five animals checked), even when the antiserum was used at a 500-fold higher concentration of anti–PAI-1 IgGs (200 μg/ml) than required to obtain a positive signal in the PAI-$1^{+/+}$ mice (0.4 μg/ml). Preadsorp-

tion of the antiserum with recombinant human PAI-1 eliminated positive staining in the wild type mice (Fig. 4 *D*). Similar data were obtained using a cross-reacting rabbit anti-human PAI-1 antiserum (data not shown).

PAI activity assays

Amidolytic assay. Similar background PAI activities were obtained in plasma from PAI-1$^{+/+}$, PAI-1$^{+/-}$, and PAI-1$^{-/-}$ mice (Table IV *A*). 4–6 h after endotoxin injection (2.0 mg/kg), PAI activity was however significantly increased in PAI-1$^{+/+}$ and PAI-1$^{+/-}$ mice, but not in PAI-1$^{-/-}$ mice.

To check whether the observed PAI activity was related to PAI-1 and not to other protease inhibitors, plasma samples of PAI-1$^{+/+}$ and PAI-1$^{-/-}$ mice were preabsorbed with a PAI-1–specific and with an irrelevant antiserum. Absorption with the PAI-1–specific antiserum, but not with the irrelevant antiserum, of plasma from endotoxin-treated PAI-1$^{+/+}$ mice reduced the PAI activity to the levels observed in plasma from untreated PAI-1$^{+/+}$ mice. Importantly, the PAI-activity levels in plasma from endotoxin-treated or untreated PAI-1$^{-/-}$ mice were not reduced after preadsorption with the PAI-1–specific antiserum. These findings suggest that the PAI activity induced with endotoxin in PAI-1$^{+/+}$ is related to PAI-1, and that the similar "baseline" activity observed in PAI-1$^{+/+}$, PAI-1$^{+/-}$, and PAI-1$^{-/-}$ mice is not related to PAI-1.

Immunofunctional assay. The immunofunctional assay for active PAI-1 levels described in Methods was developed to improve the specificity of the PAI assays for PAI-1. Baseline PAI levels were undetectable (< 2 ng/ml) in plasma from PAI-1$^{+/+}$, PAI-1$^{+/-}$, and PAI-1$^{-/-}$ mice. 4–6 h after injection of 2 mg/kg of endotoxin, an increase of the PAI-1 plasma levels over background was only observed in PAI-1$^{+/+}$ and PAI-1$^{+/-}$ mice (Table IV *B*). Preadsorption of plasma from endotoxin-treated PAI-1$^{+/+}$ mice with PAI-1–specific IgGs, but not with irrelevant IgGs, reversed the increased antigen levels to baseline. Traces of reactivated rPAI-1 added to PAI-1$^{-/-}$ plasma were quantitatively recovered, indicating that the absence of detectable active PAI-1 in plasma of PAI-1$^{-/-}$ mice was not caused by a higher degree of PAI-1 inactivation (data not shown).

^{125}I-rt-PA: PAI-1 complex formation

The reactivity of PAI in plasma of endotoxin-treated mice with rt-PA was analyzed by SDS-gel electrophoresis using ^{125}I-labeled rt-PA. Autoradiograms were overexposed to visualize the formation of trace amounts of complexes in the plasma from PAI-1$^{-/-}$ mice. When ^{125}I-rt-PA was added to plasma of endotoxin-treated PAI-1$^{+/+}$ mice (Fig. 5 *A*, lanes *1–3*), a ^{125}I-labeled complex with a similar apparent molecular weight as that obtained with mixtures of reactivated rPAI-1 and ^{125}I-rt-PA (Fig. 5 *A*, lane *5*) was observed. The formation of this complex was markedly reduced when plasma from endotoxin-treated PAI-1$^{+/+}$ mice was adsorbed with a specific PAI-1 (Fig. 5 *B*, lane *1*) but not with a control serum (Fig. 5 *B*, lane *3*). In plasma from endotoxin-treated PAI-1$^{-/-}$ mice, two very faint ^{125}I-labeled complexes with closely related relative molecular weights were observed after incubation with ^{125}I-rt-PA (Fig. 5 *A*, lane *4*). Formation of these complexes could, however, not be prevented by preadsorbing the plasma with either the PAI-1–specific (Fig. 5 *B*, lane *2*) or the control serum (Fig. 5 *B*, lane *4*), suggesting that these compounds may represent complexes of ^{125}I-rt-PA with other protease inhibitors. Plasma of endotoxin treated PAI-1$^{-/-}$ mice did not prevent the formation of the complex between ^{125}I-rt-PA and reactivated rPAI-1 added to the plasma (Fig. 5 *B*, lane *5*).

Discussion

Despite extensive characterization of the biochemical and molecular properties of PAI-1, much of our knowledge about its in

Table IV. PAI/PAI-1 Activity in Plasma

	Without endotoxin stimulation			With endotoxin stimulation		
	PAI-1$^{+/+}$	PAI-1$^{+/-}$	PAI-1$^{-/-}$	PAI-1$^{+/+}$	PAI-1$^{+/-}$	PAI-1$^{-/-}$
A. Amidolytic assays						
Plasma samples	18±2 (6)	21±2 (3)	24±2 (7)	140±9 (9)	110±7* (6)	23±7 (10)
Plasma pool						
Total	17±4	ND	17±3	130±19	ND	25±4
Adsorbed with						
anti PAI-1 IgG	18±3	ND	17±4	22±6§	ND	21±4
irrelevant IgG	19±4	ND	17±3	140±8	ND	24±3
B. Immunofunctional assays						
Plasma samples	<2 (8)	<2 (3)	<2 (8)	63±2 (11)	30±10‡ (4)	<2 (11)
Plasma pool						
Total	<2	ND	<2	56±13	ND	<2
Adsorbed with						
anti-PAI-1 IgG	<2	ND	<2	2.8±0.5§	ND	<2
irrelevant IgG	<2	ND	<2	49±12	ND	<2

Data represent mean±SEM of PAI activity levels in individual plasma samples from the number of mice indicated (plasma samples) and of duplicate measurements of PAI levels in three independent plasma pools from three to five mice (plasma pool). Plasma samples were obtained from untreated mice and from mice that received 4–6 h earlier an intraperitoneal injection of 2 mg/kg endotoxin. The plasma pool was assayed as such (total) and after absorption with PAI-1 specific and irrelevant IgGs, as described in the text. * $P < 0.05$ and ‡ $P = 0.06$ (Student's *t* test) vs plasma PAI-1levels from PAI-1$^{+/+}$ mice; § $P < 0.05$ (Student's *t* test) vs plasma from PAI-1$^{+/+}$ mice. ND, not determined.

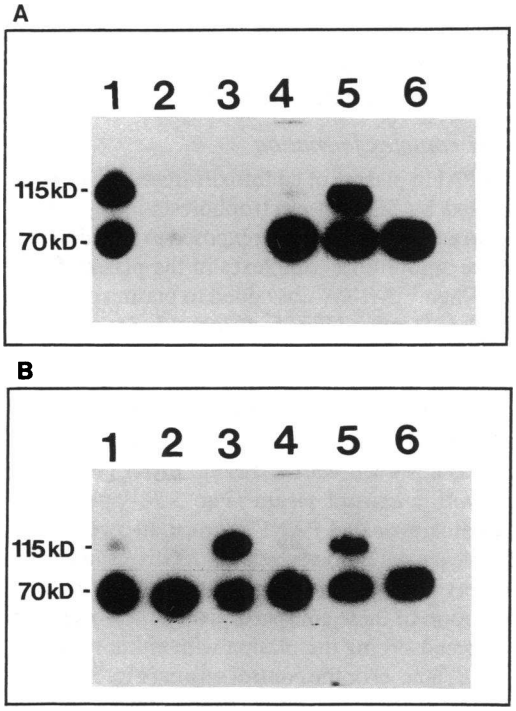

Figure 5. Autoradiogram of SDS gels of plasma of endotoxin-treated PAI-$1^{+/+}$ or PAI-$1^{-/-}$ mice, incubated with ^{125}I-rt-PA. A plasma pool of five animals was used. The autoradiogram was overexposed to visualize trace amounts. (*A*) Lanes *1–3* represent plasma of PAI-$1^{+/+}$ mice was incubated with ^{125}I-rt-PA and electrophoresed undiluted (lane *1*) or after 10-fold (lane *2*) or 100-fold dilution (lane *3*). (Lane *4*) Plasma of PAI-$1^{-/-}$ mice incubated with an equal amount of ^{125}I-rt-PA as used for incubation of plasma from PAI-$1^{+/+}$ mice, electrophoresed undiluted. (Lane *5*) Mixture of reactivated rPAI-1 and ^{125}I-rt-PA. (Lane *6*) Free ^{125}I-rt-PA. (*B*) Lanes *1–3* represent plasma from PAI-$1^{+/+}$ (lanes *1* and *3*) and PAI-$1^{-/-}$ (lanes *2* and *4*) mice, adsorbed with PAI-1–specific antiserum (lanes *1* and *2*) or irrelevant antiserum (lanes *3* and *4*) before incubation with ^{125}I-rt-PA. (Lane *5*) Plasma from PAI-$1^{-/-}$ mice to which rPAI-1 and ^{125}I-rt-PA were sequentially added. (Lane *6*) Free ^{125}I-rt-PA.

vivo role is deduced from correlation between elevated PAI-1 levels and a variety of pathological disorders.

To investigate the effect of PAI-1 gene disruption on organ development and reproduction, as well as on hemostasis, thrombosis, and thrombolysis, PAI-1–deficient mice were generated by homologous recombination in embryonic stem cells. Inactivation of the PAI-1 gene was demonstrated by Southern blot analysis, and confirmed by the absence of detectable PAI-1–specific mRNA, PAI-1–related antigen, and functional protein. The present study describes the generation of the PAI-$1^{-/-}$ mice and the consequences of PAI-1 gene disruption on organ development and reproduction. In an accompanying paper (13), the biological effects of PAI-1 gene disruption on hemostasis, thrombosis, and thrombolysis are described.

The most surprising finding of the present study was that PAI-1–deficient mice are viable, fertile, and without significant abnormalities in organogenesis and development. Although patients with low or absent PAI-1 levels have previously been described (reviewed in reference 13), it remained unknown whether PAI-1–deficient females can ovulate and support normal embryonic growth. Maternal expression of PAI-1 in the decidual cells is indeed believed to control invasion of the u-PA expressing trophoblasts (3, 8), whereas PAI-1 expression in the maternal ovarian cells around the time of ovulation, is thought to control follicular rupture (4) and remodeling of the postovulatory ovary (4). The present findings, however, demonstrate that reproduction and development proceed normally, also in the absence of PAI-1. Possibly, other protease inhibitors, such as PAI-2, α_2-antiplasmin, α_2-macroglobulin, C_1-esterase inhibitor, or α_1-antitrypsin, which are known to reduce plasminogen activation and/or plasmin activity, might compensate for PAI-1 deficiency. In view of the potential hazards of uncontrolled plasminogen activation for bleeding and tissue destruction, functional redundancy of protease inhibitors might indeed be advantageous. Another plausible explanation for the lack of major abnormalities in reproduction and development is, however, that PAI-1 deficiency in mice induces only a mild hyperfibrinolytic state, as detailed in the accompanying paper (13).

Although we did not use isogenic targeting DNA, which improves the frequency of gene targeting (31), an acceptable targeting frequency (5%; 17 out of 340 double-resistant ES colonies) was obtained. This may have been caused by the incorporation of a fairly large amount of homologous DNA sequence ($\sim$ 8 kb) into the targeting construct. In addition, three homologously recombined ES cell colonies were obtained, which also comprised one or more randomly integrated copies of the targeting construct (data not shown), and which were, therefore, discarded. It is not obvious why a number of chimeras with > 90% coat color chimerism did not transmit the inactivated PAI-1 gene. Possibly, poor germ cell chimerism despite significant coat color chimerism (19, 20) and/or sex conversion of female host embryo's by male ES cells (32) may explain the observed sterility.

It is interesting to note that disruption of the PAI-1 gene did not provoke any "spontaneous" apparent functional or histological abnormalities. It should be noted, however, that PAI-1 gene expression is highly regulated by a variety of growth factors, hormones, and cytokines involved in inflammation and tissue remodeling (12). Thus, the biological consequences of PAI-1 gene disruption might be more apparent after chronic stimulation of PAI-1 gene expression.

In conclusion, disruption of the PAI-1 gene is compatible with normal viability, development and fertility. Its consequences on the development of disease states with a disturbed coagulation/fibrinolytic balance, such as atherosclerosis, glomerulonephritis, and malignancy, need to be further explored.

Acknowledgments

The authors are grateful to Prof. F. Vandesande (Dept. Zoology, University of Leuven) for advice in the immunocytochemical experiments and for giving us access to his equipment, to Dr. L. Nelles for construction of the murine PAI-1 expression vector, to Dr. P. J. Declerck and M. Verstreken for help and advice with the immunochemical assays, to S. Janssen, S. Wyns, and S. Pollefeyt for expert technical assistance, and to E. Li, M. Rudnicki, and T. Jacks for expert advice in embryonic stem cell technology.

References

1. Astrup, T. 1978. Fibrinolysis: an overview. *In* Progress in Chemical Fibrinolysis and Thrombolysis. Vol. 3. J. F. Davidson, R. M. Rowan, M. M. Samama, and P. C. Desnoyers, editors. Raven Press, Ltd., New York. pp. 1–57.

2. Collen D., and H. R. Lijnen. 1991. Basic and clinical aspects of fibrinolysis and thrombolysis. *Blood.* 78:3114–3124.

3. Vassalli, J. D., A. P. Sappino, and D. Belin. 1991. The plasminogen activator/plasmin system. *J. Clin. Invest.* 88:1067–1072.

4. Ohlsson, M., X. R. Peng, Y. X. Liu, X. C. Jia, A. J. W. Hsueh, and T. Ny. 1991. Hormone regulation of tissue-type plasminogen activator gene expression and plasminogen activator-mediated proteolysis. *Semin. Thromb. Hemostasis.* 17:286–290.

5. Tsafriri, A., T. A. Bicsak, S. B. Cajander, T. Ny, and A. J. W. Hsueh. 1989. Suppression of ovulation rate by antibodies to tissue-type plasminogen activator and α_2-antiplasmin. *Endocrinology.* 124:415–421.

6. Strickland, S., E. Reich, and M. I. Sherman. 1976. Plasminogen activator in early embryogenesis: enzyme production by trophoblast and parietal endoderm. *Cell.* 9:231–240.

7. Qian, Z., M. E. Gilbert, M. A. Colicos, E. R. Kandel, and D. Kuhl. 1993. Tissue-plasminogen activator is induced as an immediate-early gene during seizure, kindling and long-term potentiation. *Nature (Lond.).* 361:453–457.

8. Lala, P. K., and C. H. Graham. 1990. Mechanisms of trophoblast invasiveness and their control: the role of proteases and protease inhibitors. *Cancer Metastasis Rev.* 9:369–379.

9. Rifkin, D. B., D. Moscatelli, J. Bizik, N. Quarto, F. Blei, P. Dennis, R. Flaumenhaft, and P. Mignatti. 1990. Growth factor control of extracellular proteolysis. *Cell Differ. Dev.* 32:313–318.

10. Blasi, F., and P. Verde. 1990. Urokinase-dependent cell surface proteolysis and cancer. *Semin. Cancer Biol.* 1:117–126.

11. Schneiderman, J., and D. J. Loskutoff. 1991. Plasminogen activator inhibitors. *Trends Cardiovasc. Med.* 1:99–102.

12. Loskutoff, D. J., M. Sawdey, and J. Mimuro. 1989. Type 1 plasminogen activator inhibitor. *Prog. Hemostasis Thromb.* B. Coller, editor. Bermedica Production, Columbia, MD. 9:87–115.

13. Carmeliet, P., J. M. Stassen, L. Schoonjans, B. Ream, J. J. van den Oord, M. De Mol, R. C. Mulligan, and D. Collen. 1993. Plasminogen activator inhibitor-1 gene deficient mice. II. Effects on hemostasis, thrombosis and thrombolysis. *J. Clin. Invest.* 92:2756–2760.

14. Feinberg, R. F., L.-C. Kao, J. E. Haimowitz, J. T. Queenan, Jr., T.-C. Wun, J. F. Strauss III, and H. J. Kliman. 1989. Plasminogen activator inhibitor types 1 and 2 in human trophoblasts. *Lab. Invest.* 61:20–26.

15. Denker, H. W. 1977. Implantation. The role of proteinases, and the blockage of implantation of proteinase inhibitors. *Adv. Anat. Embryol. Cell Biol.* 53:3–123.

16. Tybulewicz, V. L., C. E. Crawford, P. K. Jackson, R. T. Bronson, and R. C. Mulligan. 1991. Neonatal lethality and lymphopenia in mice with a homozygous disruption of the c-abl proto-oncogene. *Cell.* 65:1153–1163.

17. Prendergast, G. C., L. E. Diamond, D. Dahl, and M. D. Cole. 1990. The c-*myc*-regulated gene mr1 encodes plasminogen activator inhibitor 1. *Mol. Cell. Biol.* 10:1265–1269.

18. Doetschman, T. C., H. Eistetter, M. Katz, W. Schmidt, and R. Kemler. 1985. The in vitro development of blastocyst-derived embryonic stem cell lines: formation of visceral yolk sac, blood islands and myocardium. *J. Embryol. Exp. Morphol.* 87:27–45.

19. Robertson, E. J. 1987. Embryo-derived stem cell lines. *In* Teratocarcinomas and Embryonic Stem Cells: A Practical Approach. E. J. Robertson, editor. IRL Press Ltd., Oxford. pp. 71–112.

20. Bradley, A. 1987. Production and analysis of chimaeric mice. *In* Teratocarcinomas and Embryonic Stem Cells. A Practical Approach. E. J. Robertson, editor. IRL Press, Oxford. pp. 113–151.

21. Laird, P. W., A. Zijderveld, K. Linders, M. A. Rudnicki, R. Jaenisch, and A. Berns. 1991. Simplified mammalian DNA isolation procedure. *Nucleic Acids Res.* 19:4293.

22. Sambrook, J., E. F. Fritsch, and T. Maniatis. 1989. Molecular Cloning: a laboratory manual. *In* Cold Spring Harbor Laboratory Press, Cold Spring Harbor, New York.

23. Chomczynski, P., and N. Sacchi. 1987. Single-step method of RNA isolation by acid guanidinium thiocyanate-phenol-chloroform extraction. *Anal. Biochem.* 162:156–159.

24. Pannekoek, H., H. Veerman, H. Lambers, P. Diergaarde, C. L. Verweij, A. J. van Zonneveld, and J. A. van Mourik. 1986. Endothelial plasminogen activator inhibitor (PAI): a new member of the serpin gene family. *EMBO (Eur. Mol. Biol. Organ.) J.* 5:2539–2544.

25. Stanssens, P., C. Opsomer, Y. M. Mc Keown, W. Kramer, M. Zabeau, and H. J. Fritz. 1989. Efficient oligonucleotide-directed construction of mutations in expression vectors by the gapped duplex DNA method using alternating selectable markers. *Nucleic Acids Res.* 17:4441–4454.

26. Seetharam, R., A. M. Dwivedi, J. L. Duke, A. C. Hayman, H. L. Walton, N. R. Huckins, S. M. Kamerkar, J. I. Corman, R. W. Woodeshick, R. R. Wilk, and T. M. Reilly. 1992. Purification and characterization of active and latent forms of recombinant plasminogen activator inhibitor 1 produced in *Escherichia coli*. *Biochemistry.* 31:9877–9882.

27. Hekman, C. M., and D. J. Loskutoff. 1985. Endothelial cells produce a latent inhibitor of plasminogen activators that can be activated by denaturants. *J. Biol. Chem.* 260:11581–11587.

28. Verheijen, J. H., G. T. G. Chang, and C. Kluft. 1984. Evidence for the occurrence of a fast-acting inhibitor for tissue-type plasminogen activator in human plasma. *Thromb. Haemostasis.* 51:392–395.

29. Declerck, P. J., M. Verstreken, and D. Collen. 1988. An immunofunctional assay for active plasminogen activator inhibitor-1 (PAI-1). *Fibrinolysis.* 2(Suppl.):77–78.

30. Vaughan, P. J. Declerck, E. Van Houtte, M. De Mol, and D. Collen. 1992. Reactivated recombinant plasminogen activator inhibitor-1 (rPAI-1) effectively prevents thrombolysis in vivo. *Thromb. Haemostasis.* 68:60–63.

31. te Riele, H., E. R. Maandag, and A. Berns. 1992. Highly efficient gene targeting in embryonic stem cells through homologous recombination with isogenic DNA constructs. *Proc. Natl. Acad. Sci. USA.* 89:5128–5132.

32. Robertson, E. J. 1986. Pluripotential stem cell lines as a route into the mouse germ line. *Trends Genet.* 2:9–13.

33. Mansour, S. L., K. R. Thomas, and M. R. Capecchi. 1988. Disruption of the proto-oncogene *int*-2 in mouse embryo-derived stem cells: a general strategy for targeting mutations to non-selectable genes. *Nature (Lond.).* 336:348–352.